ScienSage

Journal of Advanced Scientific Research

Available online through http://www.sciensage.info

ISSN
0976-9595
Research Article

WATER VAPOURS SENSING MECHANISM BASED ON BATIO$_3$ DOPED ZNO NANOCOMPOSITE THICK FILMS SENSOR

R M Agrawal*[1], S D Charpe[2]

[1]*Department of Physics, Shri R.L.T. College of Science, Civil lines Road, Akola, Maharashtra, India*

[2]*Department of Physics, J.D. Patil Sangludkar Mahavidyalaya, Daryapur Dist. Amravati, Maharashtra, India*

**Corresponding author: agrawal195@gmail.com*

ABSTRACT

The ZnO and $BaTiO_3$ nanoparticles were synthesized by a co precipitation method. The structural and compositional characterization has been studied by using X-ray powder diffraction (XRD). The sensors are made in the form of thick film. The Surface morphologies of the prepared samples were analyzed using Field Emission Scanning electron microscopy (FE-SEM) for thick film. Further, Water vapour or humidity sensing investigations of these sensing materials were done. Our result indicates that ZnO- $BaTiO_3$ in form of thick film sensor with different molecular weight ratio was most sensitive for humidity in comparison to pristine material under same conditions. The hysteresis plot between increasing and decreasing the RH range from 30-90% RH and vice versa has been studied. The samples resistance of ZB1 decreases 10^{10} Ω to 10^{6} Ω in comparison with the pristine materials. The similar change was also observed in sensitivity.

Keywords: ZnO, BaTiO3, Humidity chamber, XRD.

1. INTRODUCTION

Humidity sensors are generally used in various fields such as medical equipment, food production and industrial and in various agricultural processes. The materials that are developed as commercial humidity sensors comprises, organic polymer films, porous ceramics, electrolytes and various composites. As compared with the other sensing materials, ceramic metal oxides have shown various rewards such as, mechanical strength, resistance to the chemical attack, thermal and physical stability and rapid response to humidity, etc. Therefore, it is necessary to give the attention on developing new sensor materials. The humidity can be measured by change in the resistance, capacitance and thermal conductance [1]. There are many materials have been investigated in view of their potential use as humidity sensing elements based on polymers, ceramics and composite materials [2-10]. Ceramic humidity sensors are to be preferred to the rest due to their thermal, physical and chemical stability [11]. The nanocrystalline materials gain much interest due to their novel structural, electrical and optical properties that significantly differ from the bulk solid state due to the influence of quantum confinement [12,13]. Humidity sensing elements based on ZnO have also been studied [14-16]. The impact of different dopant on the characteristics and parameters of ZnO-based elements and the properties of ceramic and thick film humidity sensors [17,18]. BaTiO3 has been usually used because of its wide band gap and outstanding dielectric and ferroelectric properties, infrared detectors, piezoelectric transducers, electro-optic devices, ferroelectric memories, and humidity-gas sensor [19-20].

2. EXPERIMENTAL

2.1. Synthesis of Zinc Oxide (ZnO) nanoparticle

In this, ZnO Nanoparticle were synthesized by co precipitation method, using Zinc acetate dehydrate $Zn(O_2CCH_3)_2(H_2O)_2$, sodium hydroxide as preliminary materials. Initially, 0.2M Zinc Acetate dehydrates was dissolved in 100 ml de-ionized water was ground for 15 min and then mixed with 0.02 M solution of NaOH with the help of glass rod. The mixed solution was magnetic stirred for 15 min at constant temperature and then again it was ground for 45 min. The white precipitate product was occur at the bottom. Then abundant liquid was removed and the product was washed several times with the de-ionized water and methanol to remove by products. The final product was then filtered and it was kept in a vacuum oven at 90°C for 5 hrs. The moisture will removed from the final

product. Then this dry product was calcinated at temperature 800°C for 8 hrs. In the auto controlled muffle furnace so that the impurities from product will be completely removed and get a final product of ZnO nanoparticles.

2.2. Preparation of $BaTiO_3$ nanoparticle

In preparation of Barium titanate ($BaTiO_3$) 0.25 M $Ba(NO_3)_2$ solution and 0.25 M $TiO(NO_3)_2$ solution were dissolved in 2 N nitric acid solution in a beaker. About 0.6 M tartaric acid solution was then added to under constant magnetic string. The solution heated under continuous string to its boiling point until all the liquid evaporated. About 7 gm of ammonium nitrate was added towards the ends to avoid formation of slurry. Brown fumes evolution takes places and fluffy mass were settled at the base of the beaker. The product is then dried in vacuum oven at 90°C for 2 hrs. So that moisture will removed from the final product and we will get dry product. Then this dry product was crushed into fine powder and finally this fine nanopowder of $BaTiO_3$ was calcinated at temperature 800°C for 6 hrs. in the auto controlled muffle furnace to remove the impurity form the product will be completely removed and get a final product of $BaTiO_3$ nanoparticle.

2.3. Preparation of thick films

The thick film in the form of sensor were prepared by using screen printing technique on a glass substrate. Initially, for the screen printing the thixotropic paste was formulated by mixing the sintered fine powder of pure and composite nano powder of ZnO and $BaTiO_3$ in different molecular weight ratios, a with a solution of ethyl cellulose (as 10% temporary binder) in a mixture of organic solvent such as butyl cellulose, butyl carbitol acetate and turpineol. The ratio of inorganic to organic part chemical was kept as 75:25 in formulating the paste for the screeing printing mechanism. The paste of pure and composite materials of ZnO and $BaTiO_3$ and it was screen printed on a glass substrate in the form of thick films. The prepared films were dried at 80-95°C in oven for 2hrs then the dried films are kept for fired at 500°C for 30 min in muffle furnace (Kumar make Mumbai), so that all the organic materials (in the form of binders) and organic impurities can be evaporated form the sensor material. For the surface conductance measurement the electrodes of silver paint were formed on adjacent sides of the films and again, the film were subjected to heating at 80°C for 15 min for drying the silver paint.

2.4. Characterization

2.4.1. X-ray diffraction (XRD)

The XRD pattern of pristine zinc oxide (ZnO) nanostructure synthesized by liquid phase method via co-precipitation method calcinated at 800°C as shown in Fig. 1. The crystalline nature with 2θ peak lying at (100), (002), (101), (102), (110) and (103) planes. All the peaks match well the standard hexagonal wurtize structure of zinc oxide (ZnO) with lattice constants a = b = 0.3249 nm and c = 0.5206 nm [JCPDS card no. 36-1451]. All the peaks are perfectly match with pure ZnO structure, which indicates the high purity of the obtained ZnO nanoparticle. The average crystalline size was found to be 37.32 nm calculated by Deye-Scherrer formula [21]. Fig. 2. shows the XRD pattern of pristine barium titanate ($BaTiO_3$) nanostructure by liquid phase via sol-gel method calcinated at 800°C which is shows crystalline annealed with 2θ peak lying at (100), (110), (111), (200), (210),(211) and (220) planes.

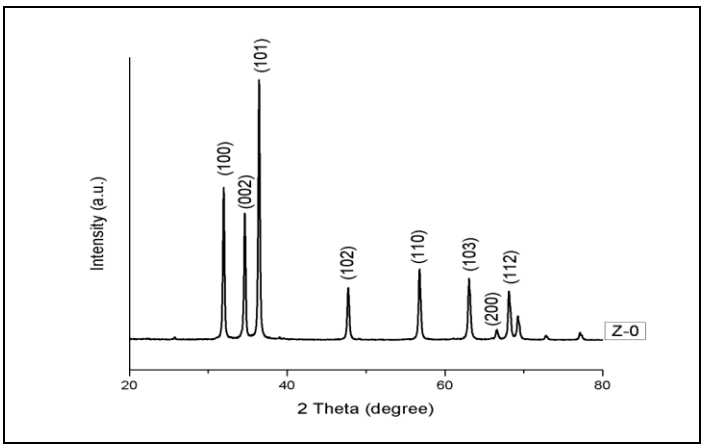

Fig. 1: XRD of pristine ZnO

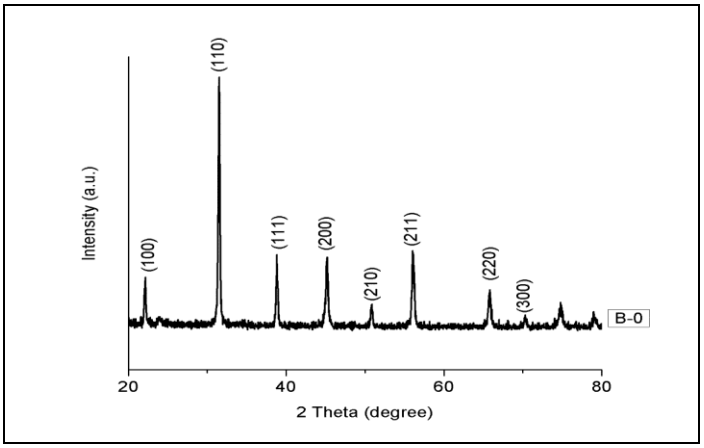

Fig. 2: XRD of pristine $BaTiO_3$

All the peaks match well with the standard provskitve type structure of barium titanate ($BaTiO_3$) with lattice constant a = 3.992 Å, c = 4.036 Å [JCPDS card no 01-075-0212]. All the peaks are perfectly match with pure $BaTiO_3$ structure which indicates high purity of the obtained $BaTiO_3$ nanoparticles. The average crystalline size was found to be 46.88 nm calculated by using Debey-Scherrer formula [22].

2.4.2. Field Emission Scanning Electron Microscopy (FE-SEM)

Fig. 3 (a) is the FE-SEM images of pure ZnO thick films. In these the particle are in both spherical and hexagonal shape with the average size 41 nm. The particle size observed in FE-SEM measurement is less than the crystalline size 56.78 nm using XRD measurement [23]. Fig. 3.(b) shows the micrograph of sample pure BaTiO3 thick films. In which the particles are found to be tetragonal shape with the average size 46 nm. The average particle size which observed in both FE-SEM were found to be nearly equal and which is greater than XRD measurement [24].

3. RESULTS AND DISCURSION

3.1. Hysteresis Plot

Hysteresis plot shows the variation between resistances of sample with respect to the relative humidity in increasing and decreasing order from 30 to 90 % RH as shown in the fig. 4. A very small hysteresis was observed during forward and reverse cycle of relative humidity, where as a very significant average change in the value of resistance of sample ZB1 (30 $BaTiO_3$- 70 ZnO) was observed the change in value of resistance is from 10^{10} Ω to 10^{6} Ω, these is a very remarkable change in the value of resistance. In the entire prepared sample the hysteresis is present which shows processes of regeneration is quite slower as compare to the other samples. A part from these a sample shows comparable decrease in resistance with an increase in % RH which indicates that the conduction occurred at the grain surface by release of electron from the water molecule. However, the sample ZB1 shows the remarkable change in the resistance values in between the humidity range 30-90 % RH and possessed a high sensitivity factor due to large surface area and porosity in the form of thick films.

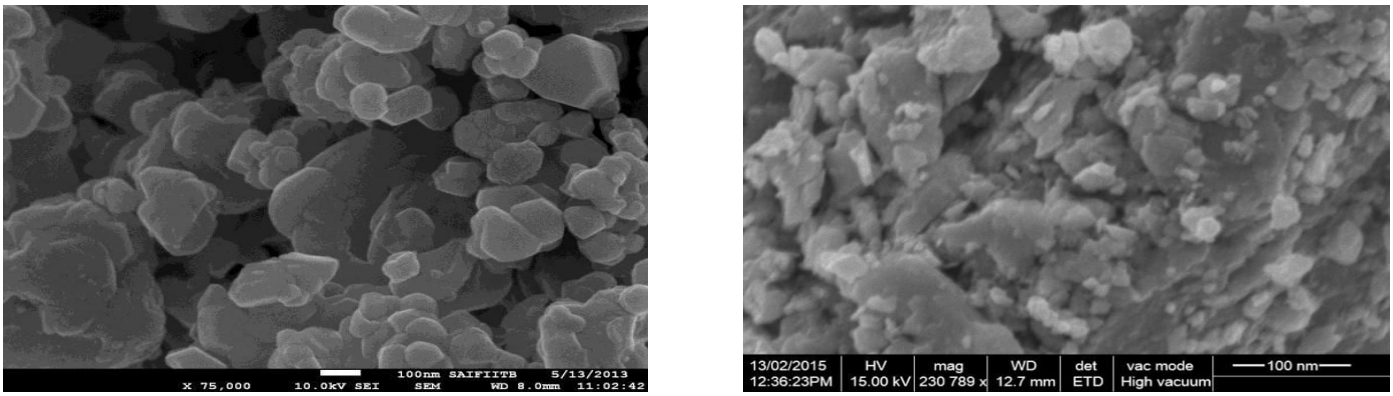

Fig. 3: SEM image of (a) ZnO and (b) $BaTiO_3$

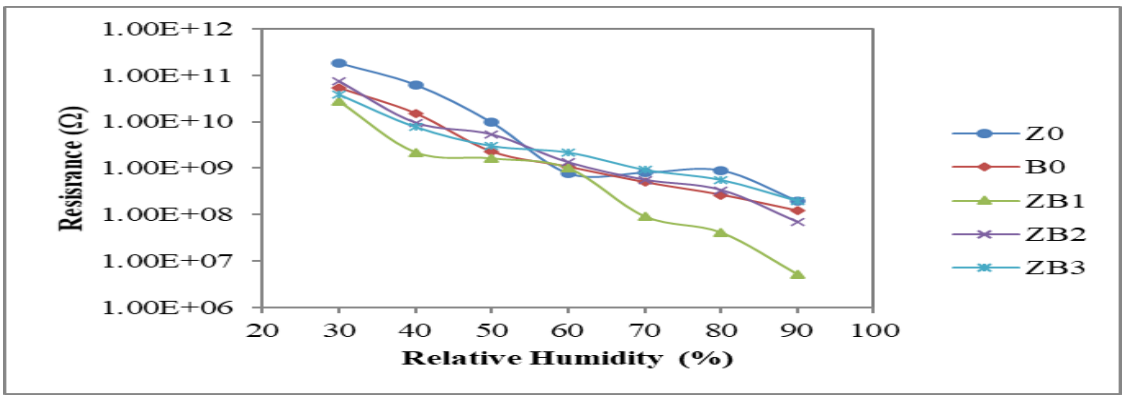

Fig. 4: Hysteresis loop

3.2. Sensitivity

In the above samples the sensitivity is found to be increasing with the RH for all the samples of thick films and it is increasing up to some particular RH and then afterward it remains constant as shown in fig. 5. For higher RH the sensitivity is found to be higher in case of all samples of thick films sensors. The sensitivity of ZB1 (30 $BaTiO_3$ -70 ZnO) is more than ZB2, ZB3 and samples and also from the pristine samples Z-0 and B-0. By addition of small amount of $BaTiO_3$ to ZnO nanoparticles which shows that the sensitivity remains constant. As previously stated that the change in conductivity is more in $BaTiO_3$ based ZnO nano composite samples the similar change is observed in sensitivity also. Hence, by the addition of $BaTiO_3$ to the pristine ZnO nanoparticles increases the sensitivity of the samples. The (ZnO-$BaTiO_3$) composite sensors exhibits significantly higher sensitivity than sensor constructed especially from ZnO, and $BaTiO_3$ nanoparticles itself due to the formation of heterogeneous interface between them and more adsorption site was created to absorbed more water vapuors [25]. The fall in resistance is mainly due to the increased amount of conduction electron or charge carrier upon adsorption of water vapours by the surface layer of the thick films.

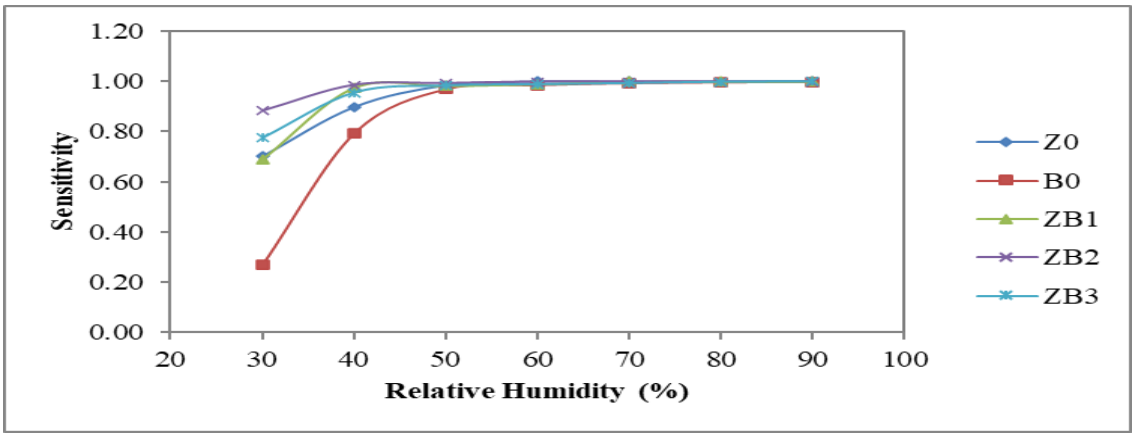

Fig. 5: Sensitivity curve

4. CONCLUSION

Nanostructured ZnO and $BaTiO_3$ were successfully prepared via co- precipitation method. Minimum crystallite size was found to be for ZnO is 37.32 nm and for $BaTiO_3$ is 46.88nm. The nano particles size crystalline i.e. the grain sizes are in the range of nanometer surface morphology was confirmed by using SEM analysis and which is responsible for humidity sensing mechanism. Surface morphology of ZB1 shows that most particles are spherical in shape leaving more space as pores and hence it will more sensitive among all the prepared samples. The Hysteresis plot shows very significant average change in the value of the resistance from 10^{10} Ω to 10^{6} Ω during forward and reversed cycles of sample ZB1. The sensitivity is found to be increasing with the RH for all the samples of thick films sensor and it is increasing up to some particular limit of RH and then afterward it remains constant. Amongst all the prepared samples ZB1 is more sensitivity than other prepared samples. This nano composites carries a good scope for the development of moisture sensor in the range of relative humidity 30% to 90% RH. The results were re- producible up to ± 77% after 2 months of observations respectively.

5. REFERENCES

1. Niranjan RS, Sathaye SD, Mulla IS. *Sensors and Actuators B*, 2007; **125:**504-509.
2. Sakai Y, Sadaoka M. *Sensors and Actuators B*, 1996; **35:**85-90.
3. Sakai Y, Matsuguchi M, Hurukawa T. *Sensors and Actuators B*, 2000; **66:**135-138.
4. Su PG, Sun YL, Lin CC. *Sensors and Actuators B*, 2006; **113:**883-886.
5. Wang J, Shi K. *Journal of Materials Science,* 2004; **39:**3155 - 3157.
6. Seiyama T, Yamazoe N, Arai H. *Sensors and Actuators B*, 1983; **4:**85-96.
7. Nenov TG, Yordanov SP. *Sensors and Actuators B*, 1992; **8:**117-122.

8. Tai WP, Oh JH. *Sensors and Actuators B*, 2002; **85:**154-157.
9. Qi QF, Zhang YT, Zheng X, Lu G. *Sensors and Actuators B*, 2009; **139:**611-617.
10. Li Y, *Talanta*, 2004; **62:**707-712.
11. Nursten H. *Journal in Food Chemistry*, 1996; **57:**481-482.
12. Das D, Pal M, Bartolomeo ED, Traversa E, Chakravorty D. *Applied. Physics*. 2000; **88:** 6856-6860.
13. Cherrey S, Tillement IO, Dubios JM. *Materials Science &Engineering A*, 2002; **338:**70-75.
14. Qi Q, Zhang T, Yu Q, Wang R, Zeng Y, Liu L, Yang H. *Sensors and Actuators B*, 2008; **133:**638-643.
15. Horzum N, Tascioglu D, Okur S, Demir M M. *Talanta*, 2011; **85:**1105-1111.
16. Yadav BC, Srivastava R, Dwivedi CD, Pramanik P. *Sensors and Actuators B*, 2008; **131:**216-222.
17. Qi Q, Zhang T, Zeng Y, Yang H. *Sensors and Actuators B*, 2009; **137:**21-26.
18. Qi Q, Zhang T, Wang S, Zheng X. *Sensors and Actuators B*, 2009; **137:**649-655.
19. Ashiri R, *Metallurgical and Materials Transactions B*, 2014; **45:**1472-1483.
20. Ashiri R, Nemati A, Ghamsari M S, Sanjabi S, Aalipour M. *Materials Research Bulletin*, 2011; **46:**2291-2295.
21. Cullity B D. Elements of X-ray diffraction. 2nd ed.: Addison-Wesley Publishing; 1978.
22. Yuk J, Troczynski T. *Sensors and Actuators B: Chemical*, 2003; **94:**290-293.
23. Chakma S, Bhasarkar J B, Moholkar V S. *International Journal of Research in Engineering and Technology*, 2013; **2:**177-183.
24. Huang TC, Wang MT, Sheu HS, Hsieh WF. *Journal of Physics: Condensed Matter*, 2007; **19:**476212.
25. Wagh MS, Patil LA, Seth T, Amalnerkar DP. *Materials Chemistry and Physics*, 2004; **84:**228-233.